M.A. Martín[1], F. San José Martínez[1] , J. Caniego[1], M. Tuller[2], A. Guber[3], Y. Pachepsky[3], C. García-Gutiérrez[1]

[1] Technical University of Madrid (UPM), Spain; [2]University of Arizona, Tucson, AZ; [3]USDA-BARC-EMSL, Beltsville, MD

Multifractal features of 3-D macropore structures of discretized X-ray CT of undisturbed soil columns

1. Objectives

1. To investigate the pore size distribution in large soil columns using CT.
2. To see whether the pore size distribution affects the saturated hydraulic conductivity of soil.

2. Soil Columns

Fig.1. Undisturbed soil core taken for the CT

Soil type: Tyler soil (fine-silty, mixed, mesic, Aeric Fragiaquults);
Location: Franklin County Pennsylvania;
Sampling depth: 0-20 cm;
Column diameter: 7.5 cm;
Clay: 26%; **Silt:** 46%; **Sand:** 28%;
Organic Carbon: 3.3%

4. Pore Size Distribution

Soil pores in columns were grouped in four size classes (Brewer, 1976). Soil pores with the size less than 0.075 mm were not detected, because of the X-ray resolution limitations, so only the macroporosity was studied. The distribution of porosity along the columns was examined for each pore class (Fig. 5). Three different types of the porosity distributions were observed, no trend with depth (e. g., Column 1); an increase in the porosity with depth (e. g., Column 3); and a decrease in the porosity with depth (Column 9). Trends were not pronounced when the porosity data from all 12 columns were combined (Fig.6). Average porosity and variability of porosity in columns generally increased with an increase in pore size, except for the coarse pore class. Overall, medium and coarse pores made up from 57% to 75% of total macroporosity in A horizon of Tyler soil.

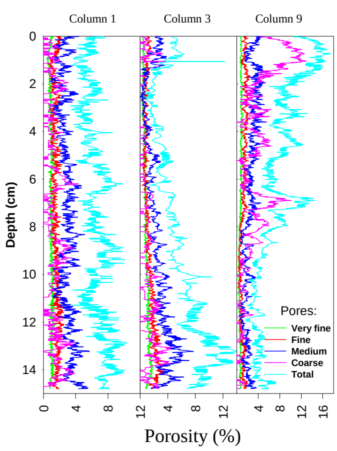

Fig.5. Distribution of soil porosity in 3 columns

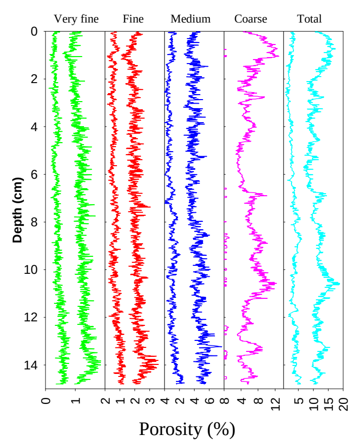

Fig.6. Range of soil porosity for each pore size in 12 columns

6. Soil Hydraulic Properties

The Column 1 was cut into 2-cm thick sections. The saturated soil conductivity K_{sat} was measured in 6 sections using constant pressure head method. Values of K_{sat} varied from 0.15 to 328 cm/h, and generally were larger in sections with the relatively high total porosity (Fig.7). The value of K_{sat} was regressed on the porosity of each pore class. Values of R^2 were substantially greater for coarse and medium pores as compared with fine and very fine pores (Fig.8). This implies that variability in the porosity of coarse and medium pores has affected variability in K_{sat}. We hypothesize that medium and coarse pores not only dominate macroporosity of the Tyler soil, but also create a continuous pore network (Fig. 4) which conducts water. However, a direct estimation of the pore connectivity is needed to evaluate the size of pores that are main water conduits.

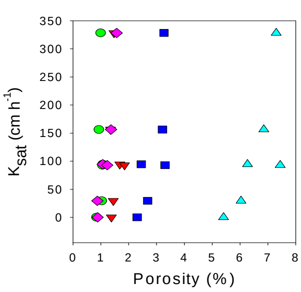

Fig. 8. Relationship between saturated hydraulic conductivity and porosity of different size classes

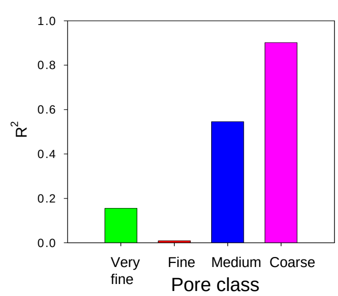

Fig. 9. Coefficients of determination for linear regressions of K_{sat} on porosity.

8. Bibliography

Brewer, 1976. R. Brewer, Fabric and Mineral Analysis of Soils. , Krieger, New York (1976).

Chun-Ming Tsai and Hsi-Jian Lee, 2002. Binarization of color document images via luminance and saturation color features. 11 (4): 434-451

J. Levy-Vehel and R.H. Riedi. 1997. *Fractional Brownian motion and data traffic modeling: The other end of the spectrum* pp 185–202, in'Fractals in Engineering' eds. Levy-Vehel, Lutton, Tricot, (Springer).

Riedi, R.H., Crouse, S., Ribeiro, V.J. and Baraniuk, R.G., 1999. A multifractal wavelet model with application to network traffic. IEEE Transactions on Information Theory, 45:992-1019.

3. Imaging and Image Processing

Twelve soil columns were scanned with the FlashCT™ - 420 kV system (HYTEC Inc.). The FlashCT-DAQ, the FlashCT-DPS, and the FlashCT-VIZ software was used for reconstruction of 1480 images in each soil column. The Median and The Fourier low pass filtering coded for Matlab (R2007) were used to reduce the artificial ring noise present at the images. The normalized cutoff frequency was set to 0.25. The images were cropped to eliminate the image parts corresponding to the acrylic container (Fig.3). The triangular Method was applied for the image binarization (Tsai and Lee, 2002). Matrox Inspector v. 4.1 (Matrox Electronic Systems Ltd.) was used to study pore size distribution in soil columns. Binarized images were used to reconstruct 3-D pore structure in the soil columns (Fig.4).

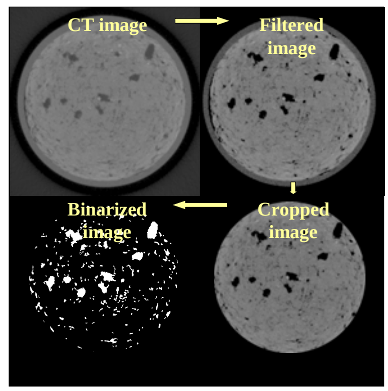

Fig.3. Image processing

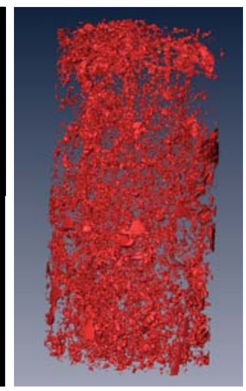

Fig.4. 3-D visualization of pore structure

5. Multifractal Analysis

The multifractal analysis has been implemented to these functions (series) by using Levi-Vehel and Riedi approach (Levy-Vehel and R.H. Riedi, 1997). Specifically, we have estimated the generalized Rényi dimensions

$$D_q \approx \frac{1}{q-1}\frac{\sum_{i=1}^{N(\varepsilon)} \mu_i(\varepsilon)^q}{\log \varepsilon}$$

where the symbol "≈" means scaling or asymptotic behavior as $\varepsilon \to 0$, $N(\varepsilon)$ is the number of interval of size ε with non zero mass and

$$\mu_i(\varepsilon) = \sum_{x_j \in I_i(\varepsilon)} \mu_j \Big/ \sum_{x_j} \mu_j$$

where the μ_i are the 2D sectional porosities for each column and the $I_i(\varepsilon)$ are subintervals of size ε

Multifractal dimensions appear well defined within a wide range of scales thus indicating the underlying multifractal structure (Fig.7).

Some dimensions might be used to infer long range dependences of soil porosity. Namely, Hurst exponents (Table 1) derived from the singularity spectrum by means of the relation (Riedi et al., 1999)

$$H = (D(2)+1)/2$$

indicate the slow decay of the correlation as a function of the distance between points (where the correlation is estimated). This is similar to the behavior of the fractional Brownian motions (fBm) with Hurst exponent between ½ and one; even if fBm are monofractals not multifractals (they have a much more simple structure that is reflected in the fact that the fBm have a spectrum reduce to a single point). This pattern sometimes has being termed as persistent. In this sense it might be related with connectivity between neighbor pores and might be correlated with hydraulic conductivity parameters.

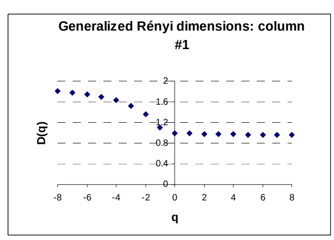

Fig.7. Generalized Rényi dimensions of the variation of 2D sectional porosity with depth

Column#	H
1	0.9896
2	0.9867
3	0.9797
4	0.9858
5	0.9860
6	0.9828
7	0.9823
8	0.9867
9	0.9828
10	0.9850
11	0.9865
12	0.9866

Table 1. Hurst parameter of the long range dependence of the variation of 2D sectional porosity with depth

7. Conclusions

1. This CT study revealed high vertical and horizontal variability in soil macroporosity.
2. Variability in soil macroporosity increased with the pore size class from very fine to medium.
3. Medium and coarse pores made up on average from 57% to 75% of the total macroporosity.
4. Vertical variability in the medium porosity and the coarse porosity caused high variability in saturated hydraulic conductivity within soil column.
5. The data provide an opportunity to study the connectivity of different pore classes and its effect on soil hydraulic properties.